

Spiro-Carbon: A Metallic Carbon Allotrope Predicted from First Principles Calculations

Felipe L. Oliveira,^[a] Rodrigo B. Capaz,^[b] and Pierre M. Esteves^{*,[a]}

A structurally stable microporous metallic carbon allotrope, poly(spiro[2.2]penta-1,4-diyne) or, for short, spiro-carbon, with I_{4h}/amd (D_{4h}) symmetry is predicted by first-principles calculations using density functional theory (DFT). The calculations of electronic, vibrational, and structural properties show that spiro-carbon has lower relative energy than other elusive carbon allotropes such as T-Carbon and 1-diamondyne (Y-Carbon). Its structure can be pictured as a set of *trans-cisoid-*

polyacetylene chains tangled and interconnected together by sp^3 carbon atoms. Calculations reveal a metallic electronic structure arising from an “intrinsic doping” of *trans-cisoid-*polyacetylene chains with sp^3 carbon atoms. Possible synthetic routes and various simulated spectra (XRD, NMR, and IR absorption) are provided in order to guide future efforts to synthesize this novel material.

1. Introduction

Pure carbon has been known since prehistorical times, becoming important for humankind throughout its existence, and being used as an energy source (coal/charcoal), materials (graphite, diamonds), beauty and social status (diamond) and even arts (char). Modernly we have rediscovered its beauty and technological potential with the rise of carbon nanotubes and graphene and this age is being considered as “The era of carbon allotropes”.^[1]

Allotropes are defined as the different structural modifications of a given element.^[2] Carbon has many known allotropes and many others are still elusive.^[3] Many of the possible allotropic structures have been compiled in the Samara Carbon Allotrope database (SACADA).^[4] We have recently reported a family of carbon allotropes called *n*-diamondynes,^[5] which are hybrids between α -carbyne and diamond, with $n = 2\alpha$. In these structures, the number of carbon atoms (α) is even, corresponding to an insertion of *n* acetylide ($-C\equiv C-$) units between the sp^3 -hybridized carbon atoms of diamond.

If one considers that 1-diamondyne, also known as Y-Carbon,^[6] could undergo rearrangements between vicinal triple bonds (as shown in Figure 1), this would result into the formation of two adjacent cyclic unsaturated three-membered rings having a single atom common to both rings, a system called a spiro compound. The resulting bicyclic system containing 5-carbon atoms is named spiropentadiene.

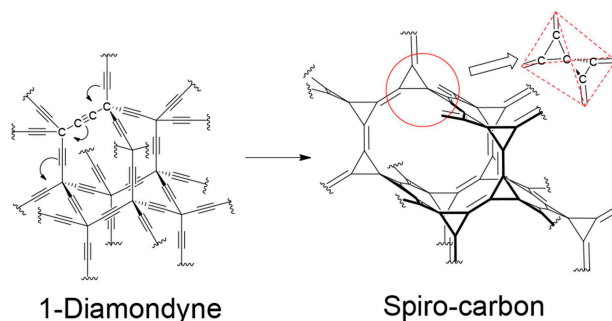



Figure 1. The rearrangement of geminal alkyne chains in 1-diamondyne (Y-Carbon), affording a carbon allotrope with the spiro-pentadiene motif.

The parent alkane, spiro-pentadiene has been already synthesized back in 1991 by Billups and Haley^[7] and it has interesting properties. For instance, its dication has already been explored in order to propose a hydrocarbon that would violate the 150-year-old paradigm that a tetravalent tetra-coordinated carbon atom must assume a tetrahedral arrangement.^[8] In neutral spiro-pentadiene, two three-member rings are orthogonal to each other, which makes this molecule actually resemble a stretched tetrahedron. As such, by periodically arranging such distorted “supertetrahedral” building blocks in an analogous way as carbon in diamond, one can potentially obtain a diamond-like carbon allotrope.

Herein we report a theoretical proposal of a carbon allotrope based on the spiro-pentadiene, which we call poly(dehydro-spiropentadiene), poly(spiro[2.2]penta-1,4-diyne) or simply spiro-carbon (Figure 2). Our calculations show that this structure is stable and has lower relative energy than other elusive carbon allotropes such as T-Carbon and 1-diamondyne (Y-Carbon). Moreover, band structure calculations indicate that it is a metal with a large density of states at the Fermi level. We also provide calculations of powder X-ray diffraction pattern, solid-state NMR chemical shifts, and IR spectra, on Supporting

[a] F. L. Oliveira, Prof. Dr. P. M. Esteves
Instituto de Química
Universidade Federal do Rio de Janeiro
Av. Athos da Silveira Ramos 149, Cidade Universitária, Rio de Janeiro, RJ
21941-909 (Brazil)
E-mail: p.esteves@iq.ufrj.br

[b] Prof. Dr. R. B. Capaz
Instituto de Física
Universidade Federal do Rio de Janeiro
Caixa Postal 68528, Rio de Janeiro, RJ 21941-972, Brazil

 Supporting information for this article is available on the WWW under <https://doi.org/10.1002/cphc.201900966>

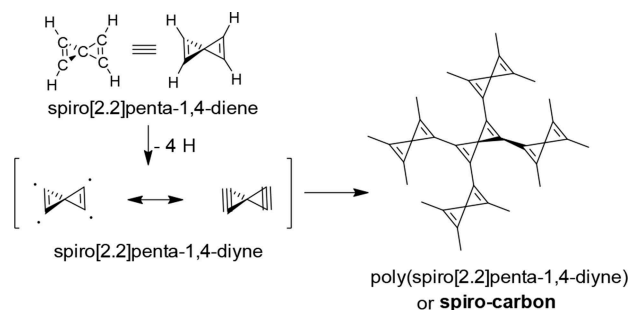


Figure 2. The chemical structures of spiropentadiene and of the poly (dehydrospiropentadiene)/spiro-carbon.

Information, that may guide future attempts to synthesize this material.

Computational Methods

Our calculations are based on DFT, as implemented in the PWscf code of Quantum ESPRESSO version 6.3.^[9,10] Exchange and correlation effects are treated with generalized gradient approximation (GGA) of Perdew-Burke-Ernzerhof (PBE) functional^[11] and electron-ion interactions are described by ultrasoft RRKJ pseudopotentials.^[12] The Kohn-Sham orbitals are expanded in a plane-wave basis set with kinetic energy cutoff of 80 Ry and 800 Ry for the charge density and the first Brillouin Zone integration was performed in a Γ -centered $12 \times 12 \times 12$ Monkhorst-Pack^[13] k -point mesh (chosen based on systematically checking the convergence with total energy). Dispersion forces were treated with D3 correction method proposed by Grimme *et al.*^[14]

Atomic positions and cell parameters were simultaneously fully optimized using the Broyden-Fletcher-Goldfarb-Shanno (BFGS) quasi-newton minimization algorithm^[15] until the Hellmann-Feynman forces acting on the atoms were lower than 10^{-5} Ry/Bohr and total energy changes less than 10^{-4} Ry.

Density of states (DOS) and projected density of states (pDOS) were calculated in a denser k -points grid of $36 \times 36 \times 36$ using the tetrahedron method^[16] for occupations. Since the system presents a metallic electronic behavior, gaussian smearing with 0.001 Ry gaussian spreading was used for Brillouin-zone integration. Phonon dispersion was calculated based on the Density-Functional Perturbation Theory approach, as implemented in the *phonon* code,^[17] with a threshold for self-consistency of 10^{-16} Ry in a q -mesh of $4 \times 4 \times 4$ and Fourier interpolated along the high symmetry points of the first Brillouin zone.

The cohesive energy, E_c , was calculated as [Eq. (1)]:

$$E_c = E_{\text{carbon}} - \frac{E_{\text{tot}}}{n_c} \quad (1)$$

where E_{tot} is the total energy of the unit cell, E_{carbon} is the energy of an isolated carbon atom on the ground state (3P_0) and n_c is the number of atoms in the unit cell. Elastic constants, C_{ij} , were obtained from the stress σ versus strain ε relation given by Hooke's Law [Eq. (2)]:

$$\sigma_c = \sum_{j=1}^6 C_{ij} \varepsilon_j \quad (2)$$

using the stress-strain routines as implemented in the thermo_pw package. The tensorial analysis of the stiffness matrix was made using the Elate tool.^[18]

The tensor for magnetic shielding was calculated based on Gauge Including Projector Augmented Wave (GIPAW) approach as implemented in the gipaw code^[19] for the Quantum Espresso package. Isotropic ^{13}C shielding, σ_{iso} , is calculated for each carbon atom as the average value of the diagonal of the calculated shielding tensor in the Principal Axis System (PAS) [Eq. (3)]:

$$\sigma_{\text{iso}} = \frac{(\sigma_{xx} + \sigma_{yy} + \sigma_{zz})}{3} \quad (3)$$

Isotropic chemical shifts (δ_{iso}) were computed following the approach of Marques *et al.*,^[20] by subtracting the σ_{iso} from the isotropic ^{13}C shielding of benzene ($\sigma_{\text{iso}}^{\text{benzene}}$), 40.6 ppm based on the equilibrium geometry, and adding the experimental isotropic chemical shift of benzene relative to tetramethylsilane (TMS) ($\delta_{\text{benzene}}^{\text{TMS}} = 126.9 \text{ ppm}$ ^[21]) to generate $\delta_{\text{iso}}^{\text{TMS}}$ [Eq. (4)]:

$$\delta_{\text{iso}}^{\text{TMS}} = -(\sigma_{\text{iso}} - \sigma_{\text{iso}}^{\text{benzene}}) + \delta_{\text{benzene}}^{\text{TMS}} \quad (4)$$

2. Results and Discussion

2.1. Geometry

The structure of spiro-carbon contains 10 carbon atoms in a body-centered tetragonal primitive cell with space group $I4_1/amd$ (space group #141) and point group D_{4h} . The resulting geometry from full variable cell optimization afforded cell parameters $a=b=5.122 \text{ \AA}$, $c=13.126 \text{ \AA}$ and $\alpha=\beta=\gamma=90^\circ$. Crystallographic information file containing the atomic coordinates are provided in the Supporting Information.

Based on the space group's symmetry of spiro-carbon, the two nonequivalent atoms occupy the Wyckoff sites 4a and 16h, being C1 on the 4a site at fractional coordinates (0.50000, 0.50000, 0.50000) and C2 on the 16h site at fractional coordinates (0.50000, 0.63609, 0.59971). According to the optimized structure it is possible to distinguish three different bond types, as outlined in Figure 3: (i) Bonds connecting the central sp^3 carbon (C1–C2) to its neighbors, with lengths 1.482 \AA , similar to the equivalent in the parent spiropentadiene (1.483 \AA – see the Supporting Information for more details) and compatible with single C–C bonds; (ii) bonds between the sp^2 carbon atoms (C2–C2) with lengths of 1.394 \AA , which is considerably larger than their corresponding bond in spiropentadiene (1.31 \AA) and present an intermediate character between single and double bond, typical of conjugated double bonds,^[22] and (iii) bonds connecting the spiro motifs to form the polymeric structure (C2=C2), with 1.342 \AA , a typical length of C=C bonds.^[22,23]

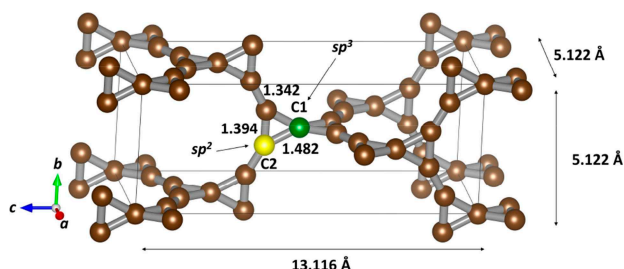


Figure 3. Atomic representation of the tetragonal structure of spiro-carbon. For simplicity, we show the conventional tetragonal (non-primitive) unit cell with two formula units. Non-equivalent C1 and C2 atoms are highlighted in green and yellow, respectively.

The angles between the two three-member rings in the spiro moiety are 90° to each other, typical of spiro compounds. The internal ring angles are 62° (C1–C2–C2 and C2–C2–C1) and 56° (C2–C1–C2). This small difference from the molecular analog, 63.6° and 52.8° respectively, is a consequence of the

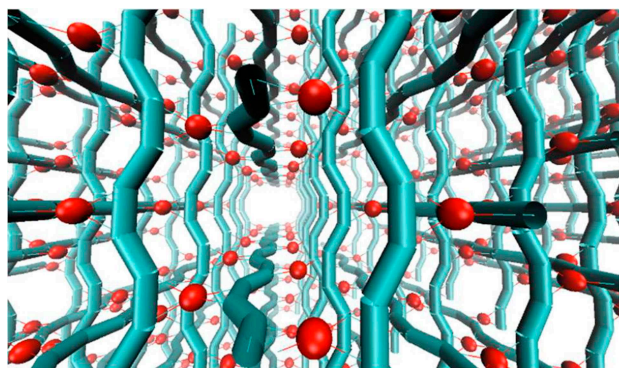
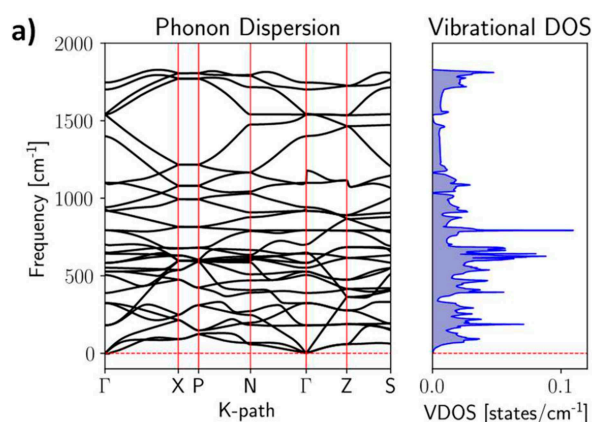


Figure 4. Schematic representation of conducting polyacetylene-like "wires", constituted by the sp^2 C2 carbon atoms (cyan), connected by the sp^3 C1 carbon atoms (red) in spiro-carbon.



changes in the length of the intra-spiro bonds (C2–C2) resulting from the formation of the periodic structure.

As can be noticed, spiro-carbon presented the double bonds outside of the three-membered ring in contrast with its molecular analog spiro-pentadiene, that exhibits inner double bonds. This contributes to a reduction of the ring strain due to longer lengths of single bonds in relation to double bonds. Moreover, this modification in the profile of the chemical bonds can have interesting consequences in the electronic structure of this new carbon allotrope, as we explore below. As we shall see, spiro-carbon can be viewed as an array of perpendicularly arranged columns of *trans-cisoid*-polyacetylene chains joined together by the sp^3 carbon atoms, as illustrated in Figure 4.

2.2. Stability and Mechanical Properties

To investigate the stability of the new proposed structure, the phonon dispersion was calculated along with the main high-symmetry directions of the first Brillouin zone^[24] (Figure S2) and it is shown in Figure 5a. The fact that no imaginary frequencies were observed in the phonon dispersion confirms that spiro-carbon structure corresponds to a minimum in the potential energy surface.

Figure 5b shows the cohesive energy versus volume (both per atom) of several carbon allotropes. As expected, the $E(V)$ curve for spiro-carbon presents a clear minimum, corresponding to a metastable state with higher energy (and therefore lower cohesive energy) than graphite or diamond. However, spiro-carbon is more stable than all other 3D carbon allotropes, such as 1-diamondyne/Y-Carbon,^[5,25] by about 2.3 kcal/mol (0.1 eV) per atom at zero pressure and T-Carbon^[26] by about 6.1 kcal/mol (0.26 eV), as shown in Table 1. This fact is remarkably encouraging, considering the recent successful synthesis of T-Carbon.^[27]

Still regarding spiro-carbon's mechanical stability, the six independent elastic constants (C_{ij} in GPa) were calculated and

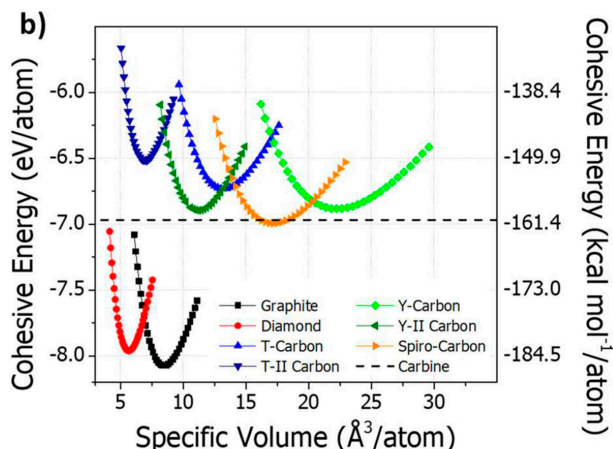


Figure 5. a) Plot of the phonon distribution along some high symmetry directions of the first Brillouin zone and the corresponding vibrational density of states (VDOS); b) Cohesive energy per atom as a function of volume per atom for different carbon allotropes. The calculation was performed considering an isotropic volume variation for all structures.

Table 1. Relative and cohesive energy, both in eV/atom, of spiro-carbon compared to different carbon allotropes.

Structure	Relative energy [eV/atom]	Cohesive energy [eV/atom]
Graphite	0.000	8.008
Diamond	0.118	7.890
Spiro-carbon	1.084	6.924
Y-Carbon	1.194	6.813
Y-II-Carbon	1.183	6.825
T-Carbon	1.347	6.660
T-II-Carbon	1.560	6.448

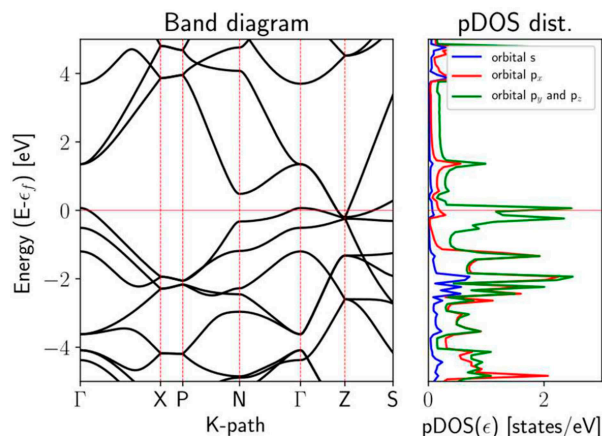
they are shown in Table 2. The four necessary and sufficient conditions that must be satisfied based on Born stability criteria to ensure mechanical stability^[28] for a tetragonal lattice are:

$$C_{11} > |C_{12}|, \quad 2C_{13} < C_{33}(C_{11} + C_{12}), \quad C_{44} > 0, \quad C_{66} < 0$$

All these criteria are completely satisfied for spiro-carbon, so we conclude that the new proposed structure is mechanically stable. A more extensive discussion of spiro-carbon elastic constants is presented in the Supporting Information.

Table 2. Elastic constants (C_{ij} in GPa), bulk (B), shear (G) and Young's (E) modulus (in GPa) and Poisson ratio (ν) calculated for Diamond, 1-Diamondyne (Y-Carbon), and Spiro-Carbon.

	Diamond	1-Diamondyne	Spiro-Carbon
C_{11}	1106.43	101.68	277.76
C_{33}	1106.43	101.68	308.54
C_{44}	591.34	13.52	75.04
C_{66}	591.34	13.52	3.61
C_{12}	153.08	79.58	3.36
C_{13}	153.08	79.58	68.88
B	470.86	86.94	123.73
G	542.45	12.47	47.79
E	1175.83	35.71	121.98
ν	0.084	0.43	0.276

**Figure 6.** Electronic band dispersion curves along high-symmetry directions of the Brillouin zone (left) and density of states (right) for spiro-carbon. Fermi level (ϵ_f) was set to 0.

2.3. Electronic Properties

As mentioned, spiro-carbon's structure resembles a set of *trans-cisoid*-polyacetylene chains in the *x*- and *y*-axis tangled and interconnected together by sp^3 carbons. Once *trans*-polyacetylene is a semiconductor, with a bandgap of approximately 1.3 eV,^[29] it would be reasonable to imagine that spiro-carbon's band structure would be reminiscent of that behavior. Intriguingly however, the analysis of the band structure (Figure 6) shows that spiro-carbon is metallic, due to the intersection between conduction and valence bands below the Fermi level near the Z point in the Brillouin zone.

The metallic character of spiro-carbon can be qualitatively understood in the following way. If spiro-carbon was composed of isolated chains of *trans-cisoid*-polyacetylene, it would be also a semiconductor. As a matter of fact, the energy difference between the valence and conduction bands at Γ is 1.28 eV, close to the calculated bandgap for the isolated *trans*-polyacetylene chain. However, the interconnection created by sp^3 carbon causes an overlap within valence and conduction bands near the Z point. As a consequence, hole pockets appear near the top of the valence band at Γ . Therefore, the metallicity of spiro-carbon can be seen as resulting from an "intrinsic doping" by the sp^3 carbon atoms, which is a rather unique effect.

The projected density of states (pDOS) (Figure 6) shows a high density of states (DOS) at the Fermi level, which is dominated by the p_y and p_z orbitals of the chains. Large peaks in the DOS are reminiscent of the quasi-1D character of the conducting chains. This suggests that spiro-carbon is a rather good metal, with a highly anisotropic conductivity (high along the chains in the *xy* directions, low along the *z* direction). Such a high DOS at the Fermi level and low-dimensional character also makes spiro-carbon prone to many-body effects such as magnetism, superconductivity or charge-density waves.

Isosurface plots of the (pseudo-)charge density calculated for the bands crossing the Fermi level at selected *k*-points (Figure 7) confirm this picture. As one can see, the electronic states at the Fermi level manifest a clear character of a π -conjugated system in the bonds between the C2 atoms.

2.4. Chemical Synthesis and Further Theoretical Characterization

The Supporting Information provides a possible synthetic route for the chemical synthesis of spiro-carbon, as well as the simulated FTIR, ^{13}C NMR isotropic chemical shifts and powder X-ray diffractogram for spiro-carbon, which can be useful information for experimental characterization of possible candidate structures. FTIR shows a main band in 918 cm^{-1} due to the E_u mode and two minor bands in 527 and 1100 cm^{-1} due to E_u and A_{2u} modes, respectively. As expected, there are two different chemical shifts for this structure: 47.0 ppm for carbon C1 and 133.6 ppm carbon C2. The simulated x-ray diffraction pattern calculated for a wavelength of 1.54059 \AA . The main peak in 18.5° is due to the (101) Bragg plane and the peaks in

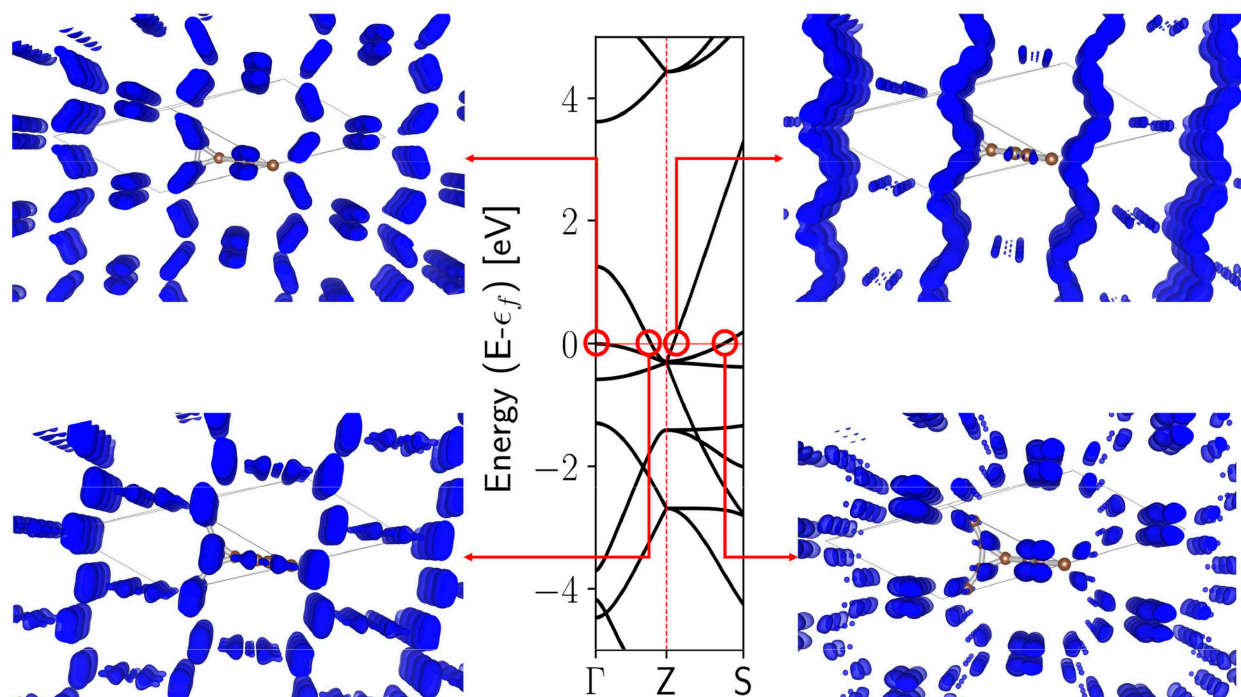


Figure 7. Band-decomposed plot of (pseudo-)charge density calculated for the bands crossing the Fermi level at selected k-points.

29.8° and 35.0° are due to the planes (112) and (200) respectively. Supporting Information section also supplies an analysis of the microporous structure of spiro-carbon, exploring its capacity for gas adsorption.

3. Conclusions

In this work, we propose a novel, unique and yet unreported carbon allotrope called spiro-carbon. Our proposal is based on DFT calculations, which show that that spiro-carbon is a minimum on the potential energy surface and mechanically stable, displaying lower formation energy than other reported carbon allotropes, such as Y-, T- and T-II-Carbon. Spiro-carbon is composed of interconnected chains of *trans-cisoid*-polyacetylene and it presents an unusual metallic electronic character. Since its parent compound, spiropentadiene was already successfully synthesized, the chances that this elusive carbon allotrope could be synthesized are considerable. The present structure actually corresponds to the 0-spiro-carbon, and acetylide units interconnecting the spiro units would afford a whole family of carbon allotropes. We hope in the future that synthetic efforts could bring this family to the real world.

Acknowledgements

We acknowledge financial support from CAPES (Project 001), INCT-Nanomateriais de Carbono, CNPq, and FAPERJ. The authors would like to thank the Núcleo Avançado de Computação de Alto

Desempenho (NACAD) of COPPE/UFRJ for the computational facility.

Conflict of Interest

The authors declare no conflict of interest.

Keywords: carbon allotrope • conductive carbon • 3D carbon allotrope • density functional calculations • nanoporous carbon

- [1] A. Hirsch, *Nat. Mater.* **2010**, *9*, 868–871.
- [2] A. D. McNaught, A. Wilkinson, *IUPAC Compendium of Chemical Terminology*, IUPAC, Research Triangle Park, NC **2009**.
- [3] R.-S. Zhang, J.-W. Jiang, *Front. Phys.* **2019**, *14*, 13401.
- [4] R. Hoffmann, A. A. Kabanov, A. A. Golov, D. M. Proserpio, *Angew. Chem. Int. Ed.* **2016**, *55*, 10962–10976; *Angew. Chem.* **2016**, *128*, 11122–11139.
- [5] D. G. Costa, F. J. F. S. Henrique, F. L. Oliveira, R. B. Capaz, P. M. Esteves, *Carbon* **2018**, *136*, 337–344.
- [6] J. Y. Jo, B. G. Kim, *Phys. Rev. B* **2012**, *86*, 075151.
- [7] W. E. Billups, M. M. Haley, *J. Am. Chem. Soc.* **1991**, *113*, 5084–5085.
- [8] P. M. Esteves, N. B. P. Ferreira, R. J. Corrêa, *J. Am. Chem. Soc.* **2005**, *127*, 8680–8685.
- [9] P. Giannozzi, S. Baroni, N. Bonini, M. Calandra, R. Car, C. Cavazzoni, D. Ceresoli, G. L. Chiarotti, M. Cococcioni, I. Dabo, A. Dal Corso, S. de Gironcoli, S. Fabris, G. Fratesi, R. Gebauer, U. Gerstmann, C. Gougousis, A. Kokalj, M. Lazzeri, L. Martin-Samos, N. Marzari, F. Mauri, R. Mazzarello, S. Paolini, A. Pasquarello, L. Paulatto, C. Sbraccia, S. Scandolo, G. Sclauzero, A. P. Seitsonen, A. Smogunov, P. Umari, R. M. Wentzcovitch, *J. Phys. Condens. Matter* **2009**, *21*, 395502.
- [10] P. Giannozzi, O. Andreussi, T. Brumme, O. Bunau, M. Buongiorno Nardelli, M. Calandra, R. Car, C. Cavazzoni, D. Ceresoli, M. Cococcioni, N. Colonna, I. Carnimeo, A. Dal Corso, S. de Gironcoli, P. Delugas, R. A. DiStasio, A. Ferretti, A. Floris, G. Fratesi, G. Fugallo, R. Gebauer, U. Gerstmann, F. Giustino, T. Gorni, J. Jia, M. Kawamura, H.-Y. Ko, A. Kokalj,

- E. Küçükbenli, M. Lazzeri, M. Marsili, N. Marzari, F. Mauri, N. L. Nguyen, H.-V. Nguyen, A. Otero-de-la-Roza, L. Paulatto, S. Poncé, D. Rocca, R. Sabatini, B. Santra, M. Schlipf, A. P. Seitsonen, A. Smogunov, I. Timrov, T. Thonhauser, P. Umari, N. Vast, X. Wu, S. Baroni, *J. Phys. Condens. Matter.* **2017**, *29*, 465901.
- [11] J. P. Perdew, K. Burke, M. Ernzerhof, *Phys. Rev. Lett.* **1996**, *77*, 3865–3868.
- [12] A. M. Rappe, K. M. Rabe, E. Kaxiras, J. D. Joannopoulos, *Phys. Rev. B* **1990**, *41*, 1227–1230.
- [13] H. J. Monkhorst, J. D. Pack, *Phys. Rev. B* **1976**, *13*, 5188–5192.
- [14] S. Grimme, J. Antony, S. Ehrlich, H. Krieg, *J. Chem. Phys.* **2010**, *132*, 154104.
- [15] B. G. Pfrommer, M. Côté, S. G. Louie, M. L. Cohen, *J. Comput. Phys.* **1997**, *131*, 233–240.
- [16] P. E. Blöchl, O. Jepsen, O. K. Andersen, *Phys. Rev. B* **1994**, *49*, 16223–16233.
- [17] S. Baroni, S. de Gironcoli, A. Dal Corso, P. Giannozzi, *Rev. Mod. Phys.* **2001**, *73*, 515–562.
- [18] R. Gaillac, P. Pullumbi, F.-X. Coudert, *J. Phys. Condens. Matter.* **2016**, *28*, 275201.
- [19] N. Varini, D. Ceresoli, L. Martin-Samos, I. Girotto, C. Cavazzoni, *Comput. Phys. Commun.* **2013**, *184*, 1827–1833.
- [20] M. A. L. Marques, M. D’Avezac, F. Mauri, *Phys. Rev. B* **2006**, *73*, 125433.
- [21] A. K. Jameson, C. J. Jameson, *Chem. Phys. Lett.* **1987**, *134*, 461–466.
- [22] D. R. Lide, *Tetrahedron.* **1962**, *17*, 125–134.
- [23] A. A. Zavitsas, *J. Phys. Chem. A* **2003**, *107*, 897–898.
- [24] C. Bradley, A. Cracknell, *The Mathematical Theory of Symmetry in Solids: Representation Theory for Point Groups and Space Groups*, OUP Oxford, **2009**.
- [25] D. Li, F. Tian, D. Duan, Z. Zhao, Y. Liu, B. Chu, X. Sha, L. Wang, B. Liu, T. Cui, *RSC Adv.* **2014**, *4*, 17364.
- [26] X.-L. Sheng, Q.-B. Yan, F. Ye, Q.-R. Zheng, G. Su, *Phys. Rev. Lett.* **2011**, *106*, 155703.
- [27] J. Zhang, R. Wang, X. Zhu, A. Pan, C. Han, X. Li, Dan Zhao, C. Ma, W. Wang, H. Su, C. Niu, *Nat. Commun.* **2017**, *8*, 683.
- [28] F. Mouhat, F.-X. Coudert, *Phys. Rev. B* **2014**, *90*, 224104.
- [29] R. H. Baughman, J. L. Bredas, R. R. Chance, R. L. Elsenbaumer, L. W. Shacklette, *Chem. Rev.* **1982**, *82*, 209–222.

Manuscript received: October 4, 2019
 Revised manuscript received: November 19, 2019
 Accepted manuscript online: November 19, 2019
 Version of record online: December 9, 2019